THE JOURNAL OF PROSTHETIC DENTISTRY

RESEARCH AND EDUCATION

Effect of machining damage on the surface roughness and flexural strength of CAD-CAM materials

Hetaf Redwan, BDS, MSc, AEED, DScD,[a] Yuwei Fan, MSc, PhD,[b] and Russell Giordano II DMD, DMSc, FADI, CAGS[c]

ABSTRACT

Statement of problem. Computer-aided design and computer-aided manufacturing (CAD-CAM) materials are available for different types of restorations. However, the longevity of the material is affected by chipping, milling damage, flexural strength, and surface roughness, and a standard edge chipping test or standardized measurements are unavailable for monitoring edge chipping of rotary instrument-milled materials.

Purpose. The purpose of this in vitro study was to analyze the surface roughness and edge chipping of different CAD-CAM diamond rotary instrument-milled dental material bars, correlate the effect of machining damage with material strength, and compare the flexural strength of rotary instrument-milled and sectioned CAD-CAM blocks.

Material and methods. Five dental CAD-CAM materials were tested: lithium disilicate glass-ceramic (IPS e.max CAD), leucite-reinforced glass-ceramic (IPS Empress CAD); feldspathic porcelain (Vitablocs Mark II); feldspar ceramic-polymer infiltrated (Enamic), and composite resin (Lava Ultimate). Rectangular bars were designed and milled for each material (n=10). The surface roughness of the bars was measured using a profilometer. All edges of 3 selected bars were analyzed with scanning electron microscopy (SEM) for the chip length, depth, and area. The 3-point bend test was used to test the flexural strength of rotary instrument-milled and saw-cut bars with the same dimensions. Analysis of variance and the Tukey honestly significant difference post hoc test were used to determine the difference among the groups (α=.05).

Results. IPS e.max CAD had the highest surface roughness and Lava Ultimate the lowest. Lava Ultimate had the smallest chipping factor and IPS Empress CAD the largest. The surface location significantly affected the chipping depth, area, and length ($P<.05$). A strong correlation was found between the decrease in flexural strength and the chipping length on the central tensile side of the rotary instrument-milled materials ($R^2=.62$, $P=.01$), as well as the chipping depth ($R^2=.44$, $P=.01$).

Conclusions. Edge chipping was significantly associated with the material type, milling surface, and edge location and strongly correlated with a decrease in flexural strength. (J Prosthet Dent 2025;133:872-880)

Computer-aided design and computer-aided manufacturing (CAD-CAM), first introduced in the 1970s,[1] is routinely used in modern prosthodontics,[2,3] with many materials being introduced,[4] including feldspathic ceramic, leucite- or lithium disilicate-reinforced glass-ceramic, and composite resin blocks.[5] IPS e.max CAD is a lithium disilicate glass-ceramic block that is available in a partially crystallized, blue state. The blue ceramic contains metasilicate and lithium disilicate nuclei, and the block is milled at the blue stage and then the restoration is crystallized with heat treatment.[6] IPS Empress CAD, introduced in 2006, is a leucite-reinforced glass-ceramic block with 1- to 5-µm leucite crystals to reinforce the crystalline matrix at a concentration of about 45% by volume.[6,7] Vitablocks Mark II is a fine-structure

All of the named authors who have been involved in the work leading to publication of this manuscript have read the paper before the submission. Authors declare there are no financial and personal relationships with other people or organizations that could inappropriately influence (bias) their work. All authors gave their final approval and agree to be accountable for all aspects of the work.

[a]Assistant Professor, Department of Restorative Dentistry, College of Dental Medicine, Umm Al-Qura University, Makkah, Saudi Arabia.
[b]Research Associate Professor, Department of Restorative Sciences & Biomaterials, Henry M. Goldman School of Dental Medicine, Boston University, Boston, Mass.
[c]Professor, Department of Restorative Sciences & Biomaterials, Henry M. Goldman School of Dental Medicine, Boston University, Boston, Mass; Assistant Dean, Biomaterials & Biomaterials Research, Henry M. Goldman School of Dental Medicine, Boston University, Boston, Mass; and Director, Biomaterials Research, Henry M. Goldman School of Dental Medicine, Boston University, Boston, Mass.

Clinical Implications

The selection of CAD-CAM restorative materials directly impacts factors such as edge chipping, milling damage, flexural strength, and surface roughness, which are influenced predominantly by the composition of the materials and milling rotary instruments.

feldspar ceramic block composed of a fine grain, (approximately 4 µm in size) feldspathic-reinforced, porcelain.[8] VITA ENAMIC material combines the properties of ceramic and polymer, consisting of a polymer-infiltrated ceramic network (PICN).[9] This material is manufactured by partially sintering ceramic particles and then infiltrating a low-viscosity polymer by capillary action. Unlike composite resins, PICNs contain 2 interconnected networks, one polymer and one ceramic.[10] Lava Ultimate is a composite resin material with a nanoparticulate prepolymerized composite resin of dispersed nanometric colloidal silica and ZrO_2 spherical particles in agglomerate and nonagglomerate form (80% by weight, 65% by volume) embedded in a dimethacrylate resin.[10–12]

The primary advantage of clinical CAD-CAM systems is to allow the clinician to fabricate restorations and prostheses from prefabricated, industrially controlled blocks of materials immediately after tooth preparation.[13–15] These systems allow the design of inlays, crowns, fixed partial dentures (FPDs), implant abutments, and other dental prostheses.[16] CAD-CAM technology has additional advantages, including digital scanning and casts, enhanced patient comfort, and the use of virtual articulators.[17] Nonetheless, the technology is expensive and requires trained personnel.[18] The milling process includes a grinding procedure to produce the 3-dimensional structure of definitive restorations.[19] Grinding can induce microcracks in the material that may reduce mechanical durability.[20,21] Further, edge chipping from the milling process may occur at the restoration margin. Edge chipping and microcracks may cause stress concentrations or even lead to restoration failure.[22,23]

The clinical longevity of restorations has been reported to be affected by edge chipping.[24–26] The purpose of this study was to analyze the effect of machining damage on the surface roughness of different CAD-CAM materials, to develop an accurate method of analyzing the edge chipping of CAD-CAM rotary instrument milled materials by measuring different parameters, and to analyze the effect of edge chipping on material strength. The authors are unaware of a standard edge chipping test or standardized measurements to monitor edge chipping for rotary instrument-milled materials. Thus, standards are needed for CAD-CAM systems to indicate a threshold of edge chipping that is associated with restoration failure. A novel concept was developed to test whether there is a correlation between edge chipping and the material strength of rotary instrument-milled bars in comparison with a control group of sectioned and polished materials. The null hypotheses tested were that no significant difference in surface roughness, edge chipping, and flexural strength would be found among different CAD-CAM materials after milling, that no significant correlation would be found between edge chipping and the flexural strength of rotary instrument milled bars of CAD-CAM materials, and that no significant difference would be found in the flexural strength of rotary instrument milled or sectioned CAD-CAM bars.

MATERIAL AND METHODS

Table 1 lists the materials used in this study. Ten rectangular bars of each material were saw cut from CAD-CAM blocks. A power analysis was performed, resulting in an estimated power >.90 with n=10. The bars were 4.0 ±0.2 mm wide, 2.0 ±0.2 mm thick, and 12.0 mm long, according to the International Organization for Standardization (ISO) 6872 standard.[27] The CAD-CAM blocks were sectioned using a precision saw (Isomet 5000; Buehler) with a continuously water-cooled diamond blade speed of 3800 RPM and a feed rate of 8.3 mm/minute. After sectioning, the bar specimens were polished with 600-grit silicon carbide abrasive paper (CarbiMet, Buehler). The IPS e.max CAD bars were polished after crystallization in a ceramic furnace (Programat CS; Ivoclar AG) at 840 °C for 7 minutes.

Rectangular bars (4×2×12 mm) were designed using a software system (SW4.2 inLab; Dentsply Sirona) shown in Figure 1. Ten bar specimens of each material were milled (CEREC inLab MC XL; Dentsply Sirona) using wet milling with a new set of diamond rotary instruments for each material. Two types of diamond rotary instruments were used: the cylinder pointed

Table 1. Materials used

Material Name	Classification	Manufacturer	Clinical Indications*
IPS e.max CAD	Lithium disilicate-based glass-matrix ceramic	Ivoclar AG	Veneers, inlays, onlays, anterior and posterior crowns, anterior and posterior implant abutments, three-unit fixed partial dentures up to premolars.
IPS Empress CAD	Leucite-based glass-matrix ceramic	Ivoclar AG	Veneers, inlays, onlays, anterior and posterior crowns.
VITA Mark II	Feldspathic glass-matrix ceramic	VITA Zahnfabrik	Veneers, inlays, onlays, anterior and posterior crowns.
Vita Enamic	Interpenetrating phase ceramic	VITA Zahnfabrik	Veneers, inlays, onlays, anterior and posterior crowns.
Lava Ultimate	Composite resin	3 M ESPE	Veneers, inlays, onlays.

* As specified by manufacturer.

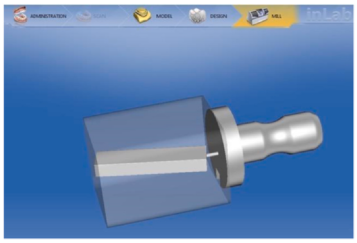

Figure 1. Bar design using inlab SW 4.2.5 software program.

rotary instrument (12S; Dentsply Sirona) and the step rotary instrument (12S; Dentsply Sirona) with a grit size of 64 μm. The cylindrical pointed rotary instrument includes 2 cutting faces 4 mm and 8 mm long and 2.1 and 1.8 mm in diameter, respectively. The step rotary instrument consisted of 3 cutting faces 3, 3, and 6 mm long and 2.1, 1.7, and 1.3 mm in diameter, respectively. Both rotary instruments were electroplated with diamond abrasives to generate flat surfaces.

Ten blocks were used for each material, as each bar was obtained from 1 block. Thereafter, 3 bars in the milling sequence of 1, 5, and 10 were selected for the edge chipping analysis using scanning electron microscopy (SEM). The milled bars had 1 surface milled only with a cylinder rotary instrument and the other surface only with a step rotary instrument. The 2 side surfaces were alternatively milled with both diamond rotary instruments. All surfaces on the bar specimens were labeled after the milling process without any surface polishing before further analysis. Thus, each labeled surface was evaluated separately for the surface roughness and SEM chipping analysis.

Roughness describes the surface texture of a material and is usually expressed by Ra, which measures the arithmetic mean of peak and valley deviation from the mean height of a surface.[28] The surface roughness of bars was measured using a profilometer (Surftest SJ-201; Mitutoyo) on all specimens. The bar specimens were placed in a custom index to hold the specimen perpendicular to the profilometer tip. The Ra value was calculated using the mean measurements at 3 longitudinal locations on each surface: 1 surface (intaglio surface for a crown) was milled with the cylinder rotary instrument and the other surface (cameo surface for a crown) was milled with the step rotary instrument. Then, a third measurement was made for each side of the bar, which was milled with both a cylinder and a step rotary instrument.

A multifactorial ANOVA test with a linear regression model was performed using a statistical software program (JMP Pro; JMP Statistical Discovery LLC) (α=.05). The model equation was expressed as: $Y=A1\times X1+A2\times X2+A3\times X1\times X2+A4$, where X1, X2 are the effect factors, and Y is the response. The Tukey HSD test was used to detect group differences (α=.05).

For the SEM analysis, each bar was mounted on an aluminum stub with carbon conductive double-sided tape (Ted Pella, Inc.). The specimens were coated with 10-nm gold-palladium (75/25) using a sputter coater (Technics Hummer V; Anatech USA), and all edges of the bar selected were analyzed sequentially with a scanning electron microscope (SU6600; Hitachi High Tech). After the edge chipping analysis, the 3 bar specimens for each material were cleaned in water in an ultrasonic bath (Quantrex LR Q140 W/T; L & R Ultrasonics) for 1 minute to remove debris, air dried, and then grouped with other bars for the flexural strength test.

The cylinder and step rotary instrument surfaces of each specimen were scanned at 3 locations: top, right, and left. The bottom edge was not included because it was affected by the removal of the bar from the block. All SEM images were made at 5 kV and ×100 magnification. The length, depth, and area of each edge chip were measured with an image processing software program (Quartz PCI ver. 9; Quartz Imaging Corp), as shown in Figure 2. The chip measurements were recorded with the corresponding milling surface (cylinder rotary instrument surface and step rotary instrument surface) and edges (top, right, and left). The chipping factor was calculated as the ratio of the sum of chip lengths to the total edge length for each edge analyzed.

The chipping analysis was conducted on the 3656 chips found on the bar specimens of all the materials tested. The chip length, area, and depth at different surface locations and in different materials were analyzed with a 1-way ANOVA and the Tukey HSD post hoc test to determine the difference between groups using a statistical software program (JMP Pro; JMP Statistical Discovery LLC) (α=.05). The chipping factor (ratio of the sum of chip lengths to total edge length), total chip length, mean chip area, and mean chip depth for every edge were also analyzed using the same method.

After milling, the IPS e.max CAD specimens were crystallized in a ceramic furnace (Programat CS; Ivoclar AG) at 840 °C for 7 minute. A 3-point bend flexural strength test with a 10 mm support span and a crosshead speed of 0.5 mm/minute was performed using a universal testing machine (Instron Model 5566A; Instron Co) following the ISO 6872 and ISO 4049 standards.[27,29]

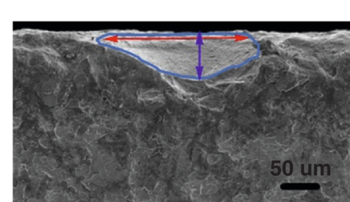

Figure 2. Representative chip measurement at top edge of IPS e.max CAD bar. *Red arrow*: chip length. *Blue arrow*: chip depth. *Blue curved area*: chip area.

As the specimen fractured, the testing software program recorded the maximum load to failure, and the flexural strength values were calculated.

The percentage of flexural strength decrease between milled and sectioned bars was calculated from

$$\textit{Flexural strength decrease} = \textit{Mean flexural strength of sectioned bar} \times 100\%$$

The flexural strength decrease was analyzed with bivariate linear regression with edge chip length, chip factor to determine the factorial correlation.

RESULTS

The mean and standard deviation were calculated for all the specimens by using the mean value of 3 measurements at the surface milled with the cylinder rotary instrument and 3 measurements at the surface milled with the step rotary instrument. One measurement was made on each side of the bar, as shown in Table 2. IPS e.max CAD had the highest surface roughness, Ra, at the bar side and step rotary instrument surfaces of 1.96 ±0.32 μm and 1.83 ±0.16 μm, respectively. Lava Ultimate had the lowest surface roughness, Ra, at the cylinder rotary instrument surface at 1.13 ±0.08 μm.

The analysis of each edge chipping measurement showed that it was associated significantly with the material type, milling surface, and edge location ($P<.05$). The means and standard deviations of the 3 measurements, chipping length, depth, and area, were calculated (Table 3). This step was performed to calculate the chipping factor of each material on both the cylinder and step rotary instrument surfaces.

The mean flexural strength for each material tested is shown in Figure 3 according to the fabrication method used (milled, sectioned). The type of material affected the mean flexural strength of rotary instrument-milled blocks significantly, in which IPS e.max CAD had the highest value (281 MPa) and Mark II the lowest (107 MPa) ($P<.05$). In comparing rotary instrument-milled versus sectioned bars, IPS e.max CAD and IPS Empress CAD showed statistically significant lower flexural strength values ($P<.001$).

The step rotary instrument surfaces demonstrated a striped milling pattern, while cylinder surfaces were more homogenous, as shown in Figure 4. The images in Figure 5, obtained using an optical surface profilometer (ZeGage; Zygo), show the different texture between the rotary instrument-milled surface with the point rotary instrument and step rotary instrument.

The decrease in the flexural strength percentage was calculated by dividing the mean flexural strength of the sectioned bar by the flexural strength of the milled bar for each material as showed in Table 4. The chipping parameters for each specimen with edge chipping of approximately 2 mm at the center of the 2 edges on the tensile side of the rectangular bar were extracted for this analysis. The results showed a strong correlation between the decrease in flexural strength and the chipping length on the central tensile side of the rotary instrument-milled materials (R^2=0.62, P=.01). The correlation between chipping and flexural strength for each material tested (Fig. 6) was positive for IPS e.max CAD (R^2=0.73), IPS Empress CAD (R^2=0.17), and Mark II (R^2=1.00), while there was no correlation for Enamic (R^2=0.02) and a negative correlation for Lava Ultimate (R^2=0.98). Further, the chipping depth was highly correlated with the decrease in flexural strength (R^2=0.44, P=.01) (Fig. 7). Other edge chipping parameters, including the chipping factor and chipping area, showed no significant correlation with the decrease in flexural strength ($P>.05$).

DISCUSSION

The null hypothesis that material type has no effect on surface roughness was rejected, as surface roughness was significantly associated with the material type and milling surface location ($P<.001$). The surface roughness Ra ranged from 1.96 μm to 1.13 μm and was greatest for

Table 2. Surface roughness of milled bars

Material/Location	Surface Roughness (Ra, μm) Mean ± Standard Deviation	Significant Difference*						
IPS e.max CAD /Side	1.96 ±0.32	A						
IPS e.max CAD /Step	1.83 ±0.16	A	B					
Mark II /Step	1.75 ±0.15	A	B	C				
IPS e.max CAD /Cylinder	1.70 ±0.13	A	B	C	D			
Enamic /Step	1.59 ±0.15		B	C	D	E		
Lava Ultimate/ Side	1.59 ±0.27		B	C	D	E	F	
Enamic /Cylinder	1.55 ±0.05			C	D	E	F	
Mark II /Side	1.50 ±0.17				D	E	F	
IPS Empress CAD / Side	1.49 ±0.10				D	E	F	
IPS Empress CAD / Step	1.45 ±0.08				D	E	F	
IPS Empress CAD / Cylinder	1.37 ±0.05					E	F	G
Enamic /Side	1.31 ±0.23						F	G
Lava Ultimate/ Step	1.18 ±0.13							G
Mark II /Cylinder	1.15 ±0.16							G
Lava Ultimate/ Cylinder	1.13 ±0.08							G

* Groups connected by same letter do not differ significantly ($P>.05$).

Table 3. Mean ±standard deviation of chip measurements in materials tested

Material Name	Surface	Total Chip Length, μm	Total Chip Area, $μm^2$	Total Chip Depth, μm
IPS e.max CAD	Cylinder	4612 ±205	155682 ±64670	1458 ±658
IPS e.max CAD	Step	4590 ±2154	192504 ±11311	1741 ±928
IPS Empress CAD	Cylinder	4612 ±1996	209387 ±116449	1699 ±836
IPS Empress CAD	Step	5533 ±3062	370231 ±242577	2179 ±1403
Enamic	Cylinder	2224 ±653	64364. ±40096	707 ±318
Enamic	Step	3989 ±2122	119477 ±78242	1427 ±898
Lava Ultimate	Cylinder	992 ±279	18465 ±7272	341 ±110
Lava Ultimate	Step	2091 ±795	42278 ±20628	760 ±347
Mark II	Cylinder	4046 ±1851	161949 ±98325	1770 ±1011
Mark II	Step	4853 ±2134	221935 ±140749	1213 ±679

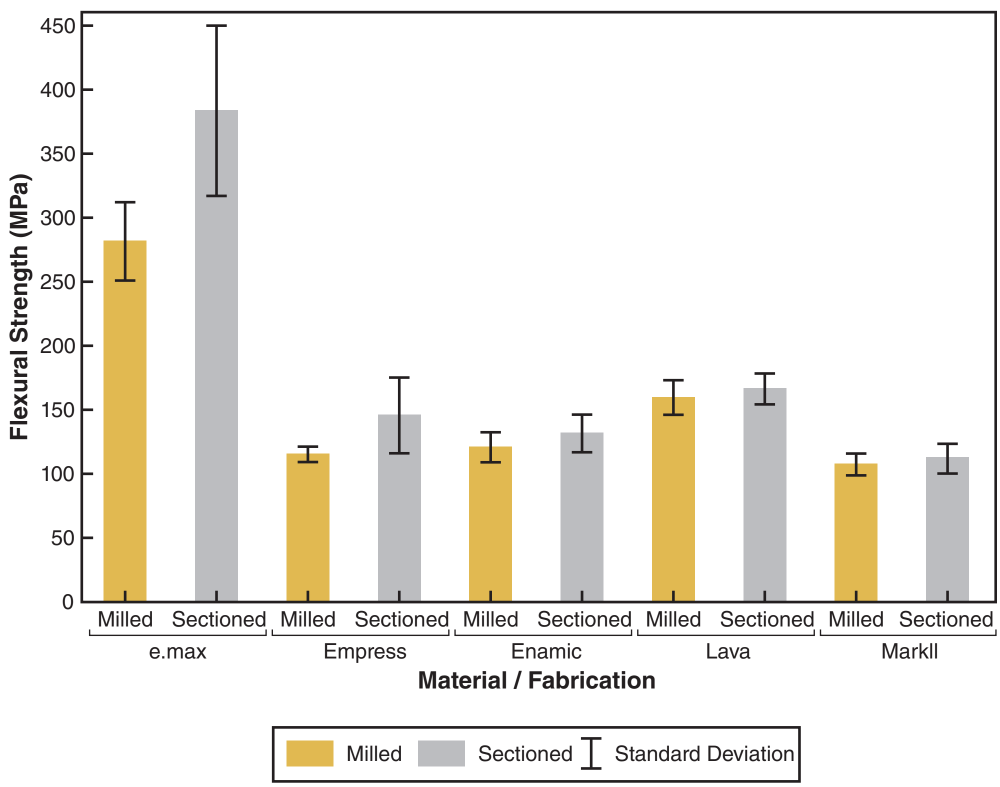

Figure 3. Mean of flexural strength of materials tested, milled versus sectioned.

lithium disilicate glass-ceramic (IPS e.max CAD), followed by interpenetrating phase ceramic (VITA Enamic), feldspathic ceramic (VITA Mark II), leucite-reinforced glass-ceramic (IPS Empress CAD), and composite resin (Lava Ultimate), respectively. For bars milled with the MC XL, 1 surface of the bar specimens was milled with a step rotary instrument and the other with a pointed cylinder rotary instrument. However, the side surfaces of the bars were milled successively with both the step and cylinder rotary instruments.

The null hypothesis that surface location has no effect on surface roughness was rejected because side and step rotary instrument surfaces had significantly higher surface roughness compared with cylinder rotary instrument surfaces. This is attributable to the rotary instrument shape, as the step rotary instrument has nearly a 90-degree angle, in contrast with the cylinder rotary instrument, which has a pointed tip that produces a smoother finish on the milled materials.[15] Further, the step rotary instrument has a wider tip that causes greater surface roughness by producing wider peaks and valleys, and a larger milling pattern than the cylinder rotary instrument, as confirmed by the optical profilometer. The milled step rotary instrument surface showed consistent straight lines with greater surface roughness, while the milled cylinder rotary instrument surface was more homogenous.

In clinical practice, CAD-CAM restorations are milled using the step rotary instrument on the intaglio surface and the cylinder rotary instrument on the cameo surface.[15] Moreover, the restoration margin is treated with both rotary instruments during milling. This milling process supports the ideal clinical goal of achieving a smooth restoration to reduce wear on opposing

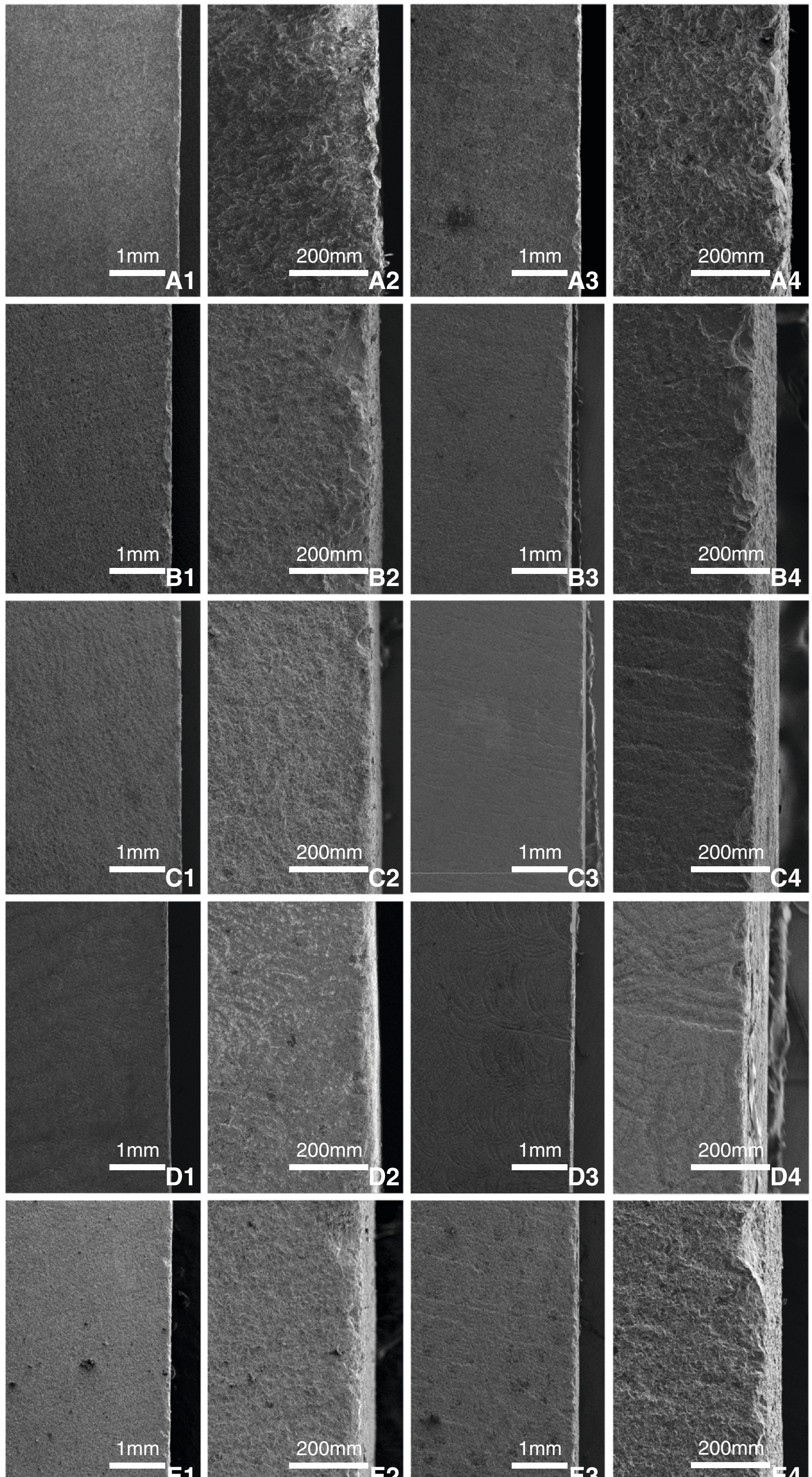

Figure 4. Scanning electron microscope images for rotary instrument-milled bars. A, IPS e.max CAD. B, IPS Empress CAD. C, Enamic. D, Lava Ultimate. E, Vitablocs Mark II. 1, cylinder rotary instrument side, original magnification ×25. 2, cylinder rotary instrument side original magnification ×100. 3, step rotary instrument side original magnification ×25. 4, step rotary instrument side original magnification ×100.

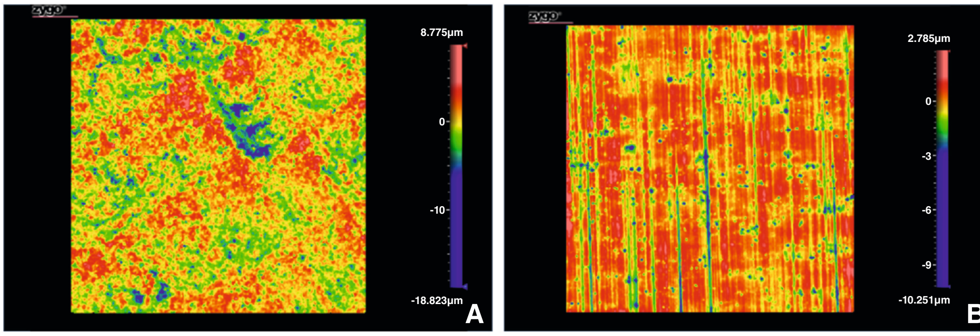

Figure 5. Optical profilometer images of IPS Empress CAD rotary instrument-milled Bar. A, Cylinder rotary instrument surface. B, Step rotary instrument surface.

Table 4. Flexural strength for milled and sectioned bars

Material	Flexural Strength of Milled Bar (MPa)*	Flexural Strength of Sectioned Bar (MPa)*	Manufacturer Flexural Strength (MPa) ISO 6872	Flexural Strength Decrease (%)
IPS e.max CAD	281.71 ±30.55 A	383.78 ±66.61 B	360	26.6%
IPS Empress CAD	115.17 ±5.89 A	145.58 ±29.66 B	160	20.8%
Enamic	120.71 ±11.76 A	131.62 ±14.74 B	150	8.3%
Lava Ultimate	159.65 ±13.46 A	166.45 ±12.06 A	204	4.0%
Mark II	107.30 ±8.60 A	111.87 ±11.62 A	154	4.0%

* Levels in same row connected by same letter do not differ significantly ($P>.05$).

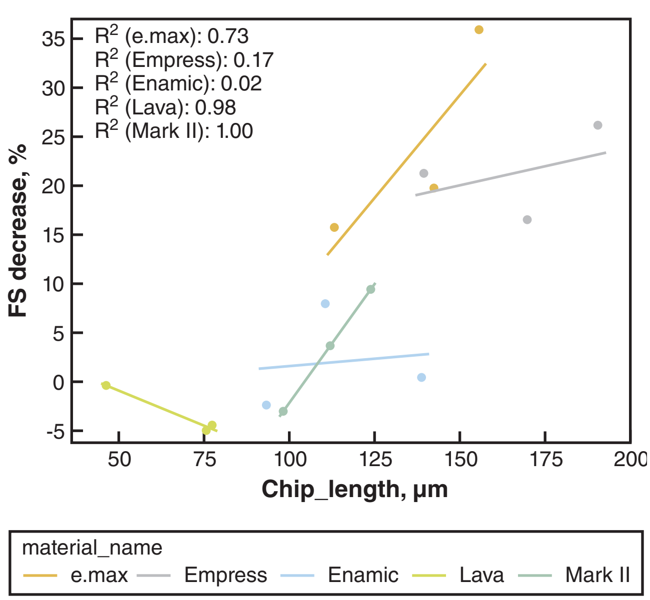

Figure 6. Correlation between flexural strength decrease and total chip length on central tensile side of 5 rotary instrument-milled materials.

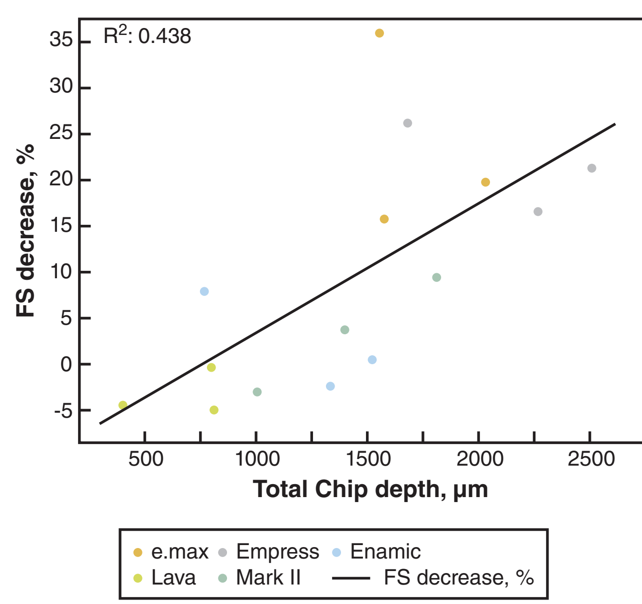

Figure 7. Correlation between flexural strength decrease and total chip depth of rotary instrument -milled materials with pooled data.

dentition, combined with a rough intaglio surface to improve cementation and bonding.[30,31]

The null hypothesis of no significant difference in edge chipping and flexural strength among different CAD-CAM materials was rejected because the edge chipping showed that ceramic materials had higher chipping factors than composite resin materials. From the SEM images, milled specimens were found to have more edge chipping compared with the sectioned bars. This result was consistent with that of Curran et al.[21]

The chipping analysis for the milled bar design showed that the material type significantly affected the chipping area, length, depth, and chipping factor. IPS Empress CAD had the greatest edge chipping in all chipping parameters, which may be attributable to the crystal size, as leucite crystal sizes range from approximately 1 to 10 µm compared with IPS e.max CAD, which has lithium disilicate crystals of approximately 2.0×7.0 µm. Although IPS e.max CAD has a high crystal content of 70% by volume, it exhibited less edge chipping than IPS Empress CAD or Vitablocs Mark II. If machining caused the crystal to pull out during the milling process, a larger chip would be seen. The lowest edge chipping was found for LAVA Ultimate, as its composite resin material contains a spherical inorganic filler of approximately 65% by volume. Further, the particle size is very small and, combined with a high polymer content, may lead the material to chip less. The polymer content appeared to help reduce the edge chipping in both LAVA Ultimate and Vita Enamic, in which the latter resists chipping because of its interconnected network combined with the small polymer content as well.

In the bar design specimens, the milled step rotary instrument surface showed significantly greater edge chipping than the milled cylinder rotary instrument surface using the 3 chipping parameters: chipping length, depth, and area. The step rotary instrument generated more edge chipping and surface roughness compared with the cylinder rotary instrument because of the difference in the rotary instrument tip design. The SEM images of these rotary instruments verified that more damage to the diamond particles was seen with the step rotary instrument causes and the rotary instrument surface texture, particularly while milling ceramic materials. The results of this study confirmed the interaction between several variables: materials; surface, and edge location. In IPS Empress CAD, the step rotary instrument surface had the highest edge chipping value, while the cylinder surface of LAVA Ultimate had the lowest value. This finding may be related to material microstructure, in which large crystals, as in IPS Empress CAD, lead to large chips.

The null hypothesis that there is no difference in the flexural strength of rotary instrument-milled or sectioned CAD-CAM bars was rejected. The results showed that the fabrication method affected the flexural strength of the glass-ceramic (IPS e.max CAD and IPS Empress CAD) significantly ($P<.05$), as the sectioned bar had greater flexural strength than the milled materials. This was attributable to the minimal edge chipping produced by the sectioning fabrication method. The sectioned specimens were polished, and SEM images confirmed that the bar edges were smooth. However, the fabrication method did not affect the flexural strength of Enamic, Lava Ultimate, or Mark II significantly ($P>.05$), likely because of the composition of Enamic and Lava Ultimate, the polymer matrices of which could absorb the energy generated by edge chipping to overcome the defects. Enamic has a dual network with an interpenetrating phase that improves the material machinability, and the small filler size in LAVA Ultimate also helps overcome the edge chipping defects and impart higher fracture toughness; therefore, it is not sensitive to edge chipping cracks.

The machining damage in IPS e.max CAD and IPS Empress CAD led to a significant drop in flexural strength compared with the sectioned bar ($P<.05$). IPS e.max CAD dropped from 383.78 MPa to 281.71, and MPa and IPS Empress CAD from 145.58 MPa to 115.17 MPa. This reduction may have been because of their high crystal content (approximately 70% by volume), which caused microcracking around the crystals; this, in turn, led to the formation of a large number of chips that lowered the material strength. IPS Empress CAD had the second greatest decrease in strength, which may be related to the large crystal size (10 µm) and high crystal content (45% by volume), which was associated with more damage and reduced strength.

The null hypothesis of no significant correlation between the edge chipping and the flexural strength of rotary instrument-milled bars of CAD-CAM materials was rejected. A strong correlation was found between the decrease in flexural strength and the increase in chipping length on the central tensile side of the rotary instrument-milled materials. The chip length at the central tensile surface of Mark II, IPS Empress CAD, and IPS e.max CAD was correlated highly with the decrease in flexural strength, which indicates that edge chipping defects in those materials affect the flexural strength significantly ($P=.023$).

The flexural strengths of sectioned CAD-CAM materials have been examined previously. The results of the present study were consistent with those of Leung et al,[4] who measured different material flexural strengths using the bar design and concluded that the flexural strength of IPS e.max CAD (341.88 ±40.25 MPa) > Vita Enamic (145.95 ±12.65 MPa) > Vitablocs Mark II (106.67 ±18.50 MPa).[4] Goujat et al[26] used a 18×3×3-mm sectioned bar design to evaluate flexural strength, and their results were also consistent with those of the present study for Vita Enamic, 148.7 MPa, and Lava Ultimate, 172.8 MPa.

Sonmez et al[11] used a 1.2×4×14-mm sectioned bar design and polished the specimens using 600-, 800-, and 1000-grit silicon carbide (SiC). They measured the flexural strength before and after thermocycling, and their flexural strength values were consistent with those of the present study. However, the milling machine caused more edge chipping in the milled bars compared with the sectioned specimens, and the flexural strength values changed accordingly.

The results in this study were consistent with those of Homaei et al,[3] who reported that the flexural strength for the sectioned bar design of IPS e.max CAD was 356.7 ±59.6 MPa and that of Vita Enamic was 135.8 ±8.3 MPa.[3] Stawarczyk et al[12] evaluated the flexural strength of a 15×4×3-mm sectioned bar polished with SiC paper P500, P1200, P2400, and P4000 and reported results consistent with those of the present study.

Limitations of the study included the in vitro design, necessary to develop an accurate method and standardization of protocols to evaluate edge chipping. Clinical studies are needed to accurately evaluate the longevity of restorative materials. Further research is recommended with different specimen designs and analyses using additional types of CAD-CAM materials after cyclic loading tests.

CONCLUSIONS

Based on the findings of this in vitro study, the following conclusions were drawn:

1. A significant difference was found between the surface roughness of machined CAD-CAM materials; IPS e.max CAD demonstrated the greatest surface roughness and Lava Ultimate the least.
2. Edge chipping was associated significantly with the type of material, milling surface, and edge location.
3. A strong correlation was found between the decrease in flexural strength and the chipping length and depth on the central tensile side of rotary instrument-milled materials.
4. Surface location affected edge chipping significantly. The step rotary instrument surface showed greater edge chipping than the cylinder rotary instrument surface.
5. Machining damage affected flexural strength, as the CAD-CAM rotary instrument-milled bars showed a significant decrease in flexural strength compared with the sectioned bars.
6. Composite resins demonstrated higher flexural strength than polymer-infiltrated ceramic and leucite-based ceramic but lower flexural strength than lithium disilicate ceramic.

REFERENCES

1. Duret F, Preston JD. CAD/CAM imaging in dentistry. *Curr Opin Dent*. 1991;1:150–154.
2. Mörmann WH. The evolution of the CEREC system. *J Am Dent Assoc*. 2006;137:7S–13S.
3. Homaei E, Farhangdoost K, Tsoi JKH, Matinlinna JP, Pow EHN. Static and fatigue mechanical behavior of three dental CAD/CAM ceramics. *J Mech Behav Biomed Mater*. 2016;59:304–313.
4. Leung BT, Tsoi JK, Matinlinna JP, Pow EH. Comparison of mechanical properties of three machinable ceramics with an experimental fluorophlogopite glass ceramic. *J Prosthet Dent*. 2015;114:440–446.
5. Giordano R. Materials for chairside CAD/CAM-produced restorations. *J Am Dent Assoc*. 2006;137:14S–21S.
6. Li RW, Chow TW, Matinlinna JP. Ceramic dental biomaterials and CAD/CAM technology: State of the art. *J Prosthodont Res*. 2014;58:208–216.
7. Guess PC, Schultheis S, Bonfante EA, Coelho PG, Ferencz JL, Silva NR. All-ceramic systems: Laboratory and clinical performance. *Dent Clin North Am*. 2011;55:333–352.
8. Charlton DG, Roberts HW, Tiba A. Measurement of select physical and mechanical properties of 3 machinable ceramic materials. *Quintessence Int*. 2008;39:573–579.
9. Goujat A, Abouelleil H, Colon P, et al. Mechanical properties and internal fit of 4 CAD-CAM block materials. *J Prosthet Dent*. 2018;119:384–389.
10. Lawson NC, Bansal R, Burgess JO. Wear, strength, modulus and hardness of CAD/CAM restorative materials. *Dent Mater*. 2016;32:e275–e283.
11. Sonmez N, Gultekin P, Turp V, et al. Evaluation of five CAD/CAM materials by microstructural characterization and mechanical tests: A comparative in vitro study. *BMC Oral Health*. 2018;18:5.
12. Stawarczyk B, Liebermann A, Eichberger M, Güth JF. Evaluation of mechanical and optical behavior of current esthetic dental restorative CAD/CAM composites. *J Mech Behav Biomed Mater*. 2015;55:1–11.
13. Chavali R, Nejat AH, Lawson NC. Machinability of CAD-CAM materials. *J Prosthet Dent*. 2017;118:194–199.
14. Beuer F, Schweiger J, Edelhoff D. Digital dentistry: An overview of recent developments for CAD/CAM generated restorations. *Br Dent J*. 2008;204:505–511.
15. Turkyilmaz I, Wilkins GN, Varvara G. Tooth preparation, digital design and milling process considerations for CAD/CAM crowns: Understanding the transition from analog to digital workflow. *J Dent Sci*. 2021;16(4):1312.
16. Tapie L, Lebon N, Mawussi B, et al. Understanding dental CAD/CAM for restorations–The digital workflow from a mechanical engineering viewpoint. *Int J Comput Dent*. 2015;18:21–44.
17. Barenghi L, Barenghi A, Garagiola U, Di Blasio A, Giannì AB, Spadari F. Pros and cons of CAD/CAM technology for infection prevention in dental settings during COVID-19 outbreak. *Sensors (Basel)*. 2021;22:49.
18. Alghazzawi TF. Advancements in CAD/CAM technology: Options for practical implementation. *J Prosthodont Res*. 2016;60:72–84.
19. Addison O, Cao X, Sunnar P, Fleming GJ. Machining variability impacts on the strength of a 'chair-side' CAD-CAM ceramic. *Dent Mater*. 2012;28:880–887.
20. Miyazaki T, Hotta Y, Kunii J, Kuriyama S, Tamaki Y. A review of dental CAD/CAM: current status and future perspectives from 20 years of experience. *Dent Mater J*. 2009;28:44–56.
21. Curran P, Cattani-Lorente M, Anselm Wiskott HW, Durual S, Scherrer SS. Grinding damage assessment for CAD-CAM restorative materials. *Dent Mater*. 2017;33:294–308.
22. Tsitrou EA, Northeast SE, van Noort R. Brittleness index of machinable dental materials and its relation to the marginal chipping factor. *J Dent*. 2007;35:897–902.
23. Vafaee F, Firooz F, Heidari B, et al. A comparative study of flexural strength and fatigue resistance of 2 nanoceramic composite resin CAM/CAM blocks (Lava Ultimate and Vita Enamic) and a lithium disilicate glass ceramic (IPS E.max CAD). *Sch J Dent Sci*. 2016;3:210–214.
24. Kern M, Sasse M, Wolfart S. Ten-year outcome of three-unit fixed dental prostheses made from monolithic lithium disilicate ceramic. *J Am Dent Assoc*. 2012;143:234–240.
25. Heintze SD, Rousson V. Survival of zirconia- and metal-supported fixed dental prostheses: A systematic review. *Int J Prosthodont*. 2010;23:493–502.
26. Scherrer SS, Quinn GD, Quinn JB. Fractographic failure analysis of a Procera all ceram crown using stereo and scanning electron microscopy. *Dent Mater*. 2008;24:1107–1113.
27. International Organization for Standardization. Dentistry - Ceramic materials. ISO Standard No. 6872,; 2015.
28. International Organization for Standardization. Geometrical product specifications (GPS) Surface texture: Profile part 2: Terms, definitions and surface texture parameters. ISO 21920-2,; 2021.
29. International Organization for Standardization, Polymer-based restorative materials, Standard No. ISO 4049, 2019.
30. Hmaidouch R, Weigl P. Tooth wear against ceramic crowns in posterior region: A systematic literature review. *Int J Oral Sci*. 2013;5:183–190.
31. Abad-Coronel C, Naranjo B, Valdiviezo P. Adhesive systems used in indirect restorations cementation: Review of the literature. *Dent J (Basel)*. 2019;7:71.

Corresponding author:
Dr Yuwei Fan
72 E Concord Street, R-520
Boston, MA 02118
Email: yuweifan@bu.edu

CRediT authorship contribution statement

Russell Giordano II: Project administration, Conceptualization, Supervision, Writing – review and editing. **Yuwei Fan**: Conceptualization, Project administration, Software, Methodology, Investigation, Formal analysis, Visualization, Writing – review and editing. **Hetaf Redwan:** Methodology, Data curation, Investigation, Formal Analysis, Writing – original draft, Writing – review and editing.

https://doi.org/10.1016/j.prosdent.2024.07.045